



# Preparation of Pd (0) and Pd (II) nanotubes and nanoparticles on modified bentonite and their catalytic activity in oxidation of ethyl benzene to acetophenone

M. Ghiaci<sup>a,\*</sup>, Z. Sadeghi<sup>b</sup>, M.E. Sedaghat<sup>a</sup>, H. Karimi-Maleh<sup>a</sup>, J. Safaei-Ghomi<sup>b</sup>, A. Gil<sup>c</sup>

<sup>a</sup> Department of Chemistry, Isfahan University of Technology, Isfahan 8415683111, Iran

<sup>b</sup> Department of Chemistry, Faculty of Sciences, University of Kashan, Kashan, Iran

<sup>c</sup> Department of Applied Chemistry, Building Los Acebos, Public University of Navarra, Campus of Arrosadia, E-31006 Pamplona, Spain

## ARTICLE INFO

### Article history:

Received 25 February 2010

Received in revised form 26 March 2010

Accepted 29 March 2010

Available online 4 April 2010

### Keywords:

Palladium

Modified bentonite

Ethylbenzene

Oxidation

## ABSTRACT

The synthesis and application of palladium nanotubes and nanoparticles on modified bentonite was studied. In the first step, an organo-bentonite was prepared by the exchange of the exchangeable Na<sup>+</sup> cations of a homoionic Na-bentonite by cetyl pyridinium cations (CP-bentonite), especially in the range of low coverage ratios where surfactant ions are adsorbed through cation exchange with the counter ions of bentonite. At this stage, there will be a disordered liquid-like monolayer arrangement of alkyl chain within the gallery. This modified bentonite was loaded with the first generation of amidamine hyperbranch cascade, 3,3'-(dodecylazanediy) bis(N-(2-(2-aminoethylamino)ethyl)propanamide) (DAEP), which has a long aliphatic tail (C<sub>12</sub>) and a hydrophilic head. The solid/liquid interfacial layer of this architecturally designed bentonite (DAEP-bentonite) was utilized as a nanoreactor for the synthesis of nanoparticles of Pd<sup>2+</sup> and Pd<sup>0</sup>. The structure, specific surface area, and porosity of bentonite are significantly altered by the incorporation of nanoparticles. These alterations were monitored by several techniques such as N<sub>2</sub> adsorption, X-ray diffraction (XRD), transmission electron microscopy (TEM) and electrochemical impedance spectroscopy (EIS). The size of the palladium nanoparticles prepared in this work was in the range of 5–15 nm. Solvent free oxidation of ethyl benzene using tert-butyl hydroperoxide as an oxidant showed that the palladium nanocatalysts prepared in this work, were highly active and selective.

© 2010 Elsevier B.V. All rights reserved.

## 1. Introduction

In the last decade, new directions of modern research, broadly defined as *nanoscale science and technology*, have emerged [1,2]. These new trends involve the ability to fabricate, characterize, and manipulate artificial structures, whose features are controlled at the nanometer level. They embrace areas of research as diverse as engineering, physics, chemistry, materials science, and molecular biology [3]. Research in this direction has been triggered by the recent availability of revolutionary instruments and approaches that allow the investigation of material properties with a resolution close to the atomic level. Strongly connected to such technological advances are the pioneering studies that have revealed new physical properties of matter at a level intermediate between atomic/molecular and bulk [4].

Nanoparticles possess unique physical and chemical properties different from bulk materials due to drastic reduction of particle size. Among those nanoparticles, palladium and its alloy nanopar-

ticles have been successfully applied to catalyze various chemical reactions. Supported noble metals catalysts are widely used in industrial processes such as chemical synthesis, oil refining and exhaust gas treatment [5].

Nanosized noble metal particles (e.g. Pt, Pd, Rh and Ru) dispersed on high surface area supports (e.g. Al<sub>2</sub>O<sub>3</sub>, SiO<sub>2</sub> and clay) have demonstrated high oxidation activity, good thermal stability and selectivity [6–9]. In 1993, Balogh and Laszlo applied clays in heterogeneous systems as catalysts or catalyst supports [10]. In 1999, Dekany and his co-workers developed preparation of palladium nanoparticles on the surface of modified clays [11].

We have reported the synthesis of nanocrystalline semiconductors (CdS, ZnS) on the surface of hydrophobized Na-bentonite [12]. In the present work, and in continuation of our research interest on modification of solid supports [13–15], the adsorption layer of modified bentonite at the solid/liquid interface was utilized as a nanophase reactor for preparation of nanocatalysts of Pd and for their stabilization. The main point of the procedure, as described deeply by Dekany et al. [11], was to modify the surface in such a way that it could adsorb the active precursor, and especially the noble metals in the adsorption layer of the surface of solid particles dispersed in a liquid medium. In this work we have made a com-

\* Corresponding author. Tel.: +98311 391 3254; fax: +98311 391 2350.

E-mail address: [mghiacy@cc.iut.ac.ir](mailto:mghiacy@cc.iut.ac.ir) (M. Ghiaci).

parison between a modified bentonite with hydrophobic nature, and a bentonite which was modified in two steps: in the first step, with a cationic surfactant (cetyl pyridinium bromide, CP) which form a disordered liquid-like monolayer arrangement of surfactant in the gallery, and in the second step with the first generation of an amidoamine cascade, named 3,3'-(dodecylazanediyl) bis(N-(2-(2-aminoethylamino)ethyl)propanamide) (DAEP) that adsorbs as a nonionic surfactant on the hydrophobized bentonite, through Van der Waals interactions. We used *n*-hexane as the dispersion medium because the precursor ions are practically insoluble in it. When solubility in the liquid phase is poor, it is expected that the precursor ions are preferentially adsorbed on the solid surface and their concentration within the bulk phase will be close to zero. With this strategy in our mind, the objective of our study was to experimentally investigate the effect of the modified bentonites on the size of the nanoparticles generated on the surface, and the catalytic activity of the resulting immobilized palladium nanoparticles in oxidation of ethyl benzene.

The aromatic ketones are important starting materials for many organic reactions, some of which find also industrial applications. The usual way for their production is Friedel–Crafts acylation by acid chlorides or anhydrides in the presence of acid catalysts of Brønsted or Lewis type. The present demand for cleaner chemical processes requires the use of environmentally friendly catalysts avoiding the evolution of aggressive gases or corrosive solutions. The palladium nanoparticles present a promising future for the Friedel–Crafts reactions. We herein report the use of Pd nanoparticles immobilized on modified bentonite as catalyst in the oxidation of ethyl benzene using *t*-butyl hydroperoxide as oxidant for production of acetophenone.

## 2. Experimental

### 2.1. Materials

The parent bentonite had the following chemical composition (in wt%): SiO<sub>2</sub> (65.04), Fe<sub>2</sub>O<sub>3</sub> (1.67), MgO (1.87), Al<sub>2</sub>O<sub>3</sub> (13.61), CaO (2.01), TiO<sub>2</sub> (0.19), Na<sub>2</sub>O (2.26), K<sub>2</sub>O (0.75). It was obtained from Salafchegan mine (Salafchegan, Iran). Cetyl pyridinium bromide (CP), methyl acrylate, dodecylamine, and diethylene triamine were purchased from Merck and used as received. The metal precursor PdCl<sub>2</sub> (purity 99%) was obtained from Aldrich. All other chemicals used in this study were of analytical grade.

### 2.2. Characterization techniques

X-ray powder diffraction was performed on a Phillips diffractometer with CuK $\alpha$  radiation (40 kV, 30 mA) over a  $2\theta$  range between 3 and 80°.

Scanning electron micrographs were obtained using a Cambridge Oxford 7060 Scanning Electron Microscope (SEM) connected to a four-quadrant backscattered electron detector with resolution of 1.38 eV. The samples were dusted on a double sided carbon tape placed on a metal stub and coated with a layer of gold to minimize charging effects.

Transmission electron microscopy (TEM) was carried out on the powder samples with a Tecnai F30 TEM operating at an accelerating voltage of 300 kV. In addition, energy dispersive X-ray analysis was conducted on each sample.

The solid-state UV–vis spectra were recorded using a PerkinElmer model Lambda 650 spectrophotometer.

BET surface area and pore size distribution were measured on a Micromeritics Digisorb 2600 system at –196 °C using N<sub>2</sub> as adsorbate. Before measurements, the samples were degassed at 450 °C for 3 h under vacuum (0.1333 Pa).

FTIR spectra of the catalyst were recorded on a JASCO FTIR 680 plus spectrometer with the KBr pellet method.

### 2.3. General procedures

#### 2.3.1. Synthesis of 3,3'-(dodecylazanediyl)bis(N-(2-(2-aminoethylamino)ethyl)propanamide) (DAEP)

Methyl acrylate (3 mmol) was added slowly to a stirred solution of dodecylamine (1 mmol) in dry CH<sub>3</sub>OH (20 mL). After stirring for 24 h at reflux temperature under nitrogen atmosphere, the solution was evaporated giving 3,3'-(dodecylazanediyl)dipropionate, (I), which was used in the subsequent step without need for purification. In the next step, diethylenetriamine (DETA) (5.25 mmol) was slowly added to 1.75 mmol of 3,3'-(dodecylazanediyl)dipropionate (I) in dry CH<sub>3</sub>OH (20 mL), and the mixture was left stirring under N<sub>2</sub> at reflux temperature for 4 days. The solution was poured into water, the solid residue dissolved in chloroform and the organic extract was dried (MgSO<sub>4</sub>) and evaporated affording 3,3'-(dodecylazanediyl)bis(N-(2-(2-aminoethylamino)ethyl)propanamide) (DAEP) (II) (Scheme 1). The product was characterized using FTIR, <sup>1</sup>H NMR, CHN and mass spectrometry. Yield 78%, m.p. 38 °C. IR (KBr):  $\nu_{\text{max}}/\text{cm}^{-1}$ , 3553 (m), 3413(w), 1657(m), 1589(s). <sup>1</sup>H NMR (CDCl<sub>3</sub>):  $\delta$  (ppm), 0.60 (CH<sub>3</sub>, 3H), 0.98 (CH<sub>2</sub>, 2OH), 1.20 (NH<sub>2</sub>, NH, 6H), 1.53 (CH<sub>2</sub>, 12H), 2.05 (CH<sub>2</sub>, 2H), 2.42 (CH<sub>2</sub>, 4H), 2.44 (CH<sub>2</sub>, 2H), 2.53 (CH<sub>2</sub>, 4H), 2.57 (CH<sub>2</sub>, 2H), 4.65 (NH, 2H). Elemental analysis % calculated for C<sub>26</sub>H<sub>57</sub>N<sub>7</sub>O<sub>7</sub>, C = 62.48, H = 11.50, N = 19.62 and observed % was C = 62.43, H = 11.57, N = 19.70. Mass (*m/z*): 499.

#### 2.3.2. Purification and modification of bentonite

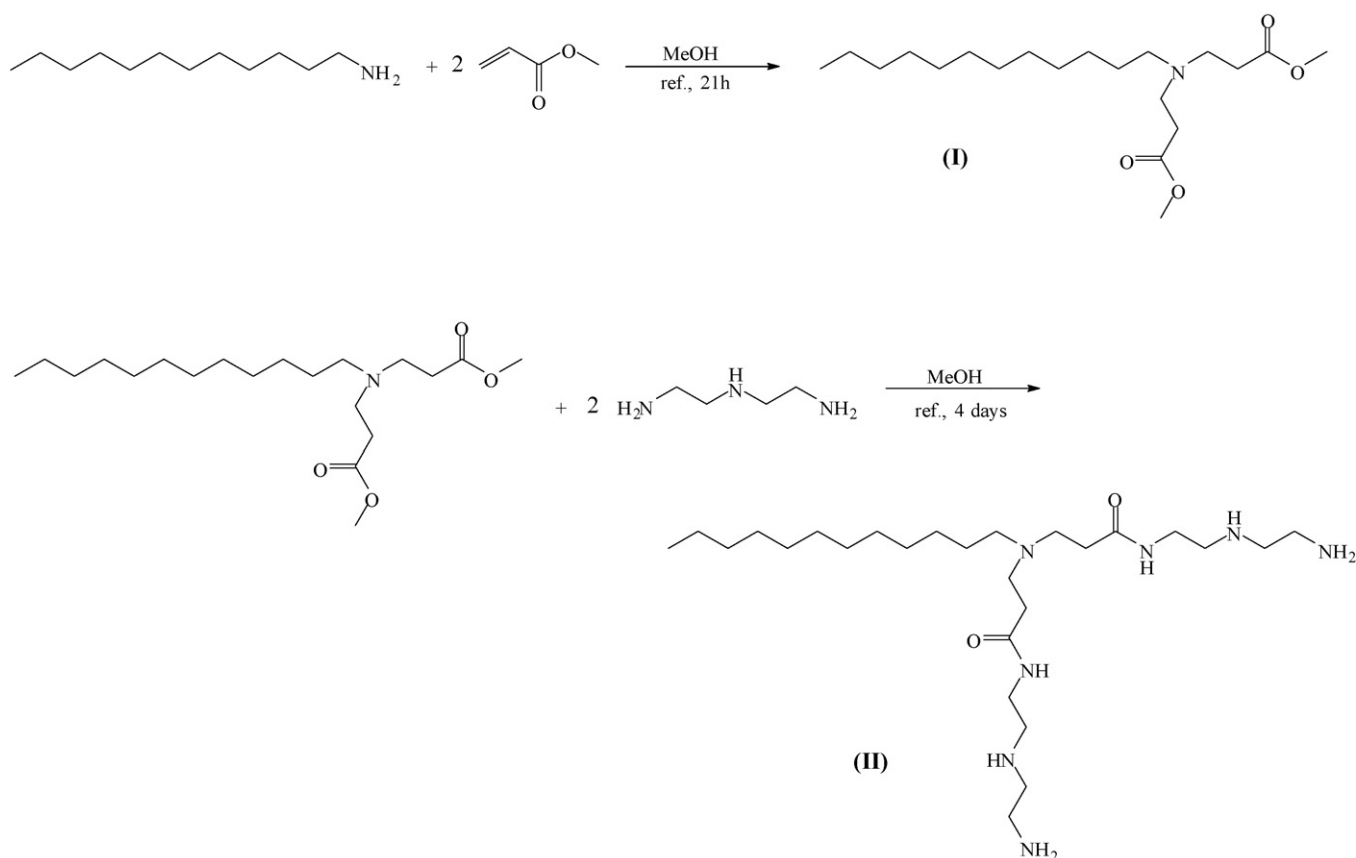
Since the XRD analysis revealed the presence of significant amount of quartz and feldspar, the raw material was purified using the following procedure. Bentonite (5% by mass), was dispersed in water under continuous stirring. After separation of quartz and feldspar, 1 M NaCl solution was added. The suspension was stirred overnight followed by decantation. The solid was washed until a negative test for chloride in solution was obtained. The cation-exchange capacity (CEC) of the Na–bentonite was measured (0.70 mequiv. g<sup>–1</sup>), by the method of Ming and Dixon [16].

In order to modify the bentonite, on the basis of the critical micelle concentration of the 3,3'-(dodecylazanediyl)bis(N-(2-(2-aminoethylamino)ethyl)propanamide) (DAEP), this surfactant was loaded on the bentonite to obtain surfactant modified bentonite (DAEP–bentonite). 1 g of Na–bentonite was dispersed in 100 mL of DAEP solution (20%, w/w, ethanol–water) (Scheme 2). The dispersion was stirred at 200 rpm for 24 h and centrifuged. The solid was washed with water to remove excess surfactant and surfactant loosely attached to the bentonite particles.

#### 2.3.3. Preparation of immobilized palladium (II) and Pd (0) on modified bentonites

In a typical experiment to prepare Pd (II)–bentonite composite, 500 mg of the monolayer surfactant coverage modified bentonite (DAEP–bentonite), was dispersed in 100 mL of *n*-hexane, to which 100  $\mu$ L of 10<sup>–2</sup> M aqueous solutions of PdCl<sub>2</sub> were added in 10 steps (each step 10  $\mu$ L) to the suspension during 72 h, under vigorous stirring in a Morton flask. The resulting product was separated via centrifugation, and washed few times with distilled water. The product was dried under vacuum at room temperature before characterization and catalytic activity measurements.

Chemical reduction of Pd (II) loaded on modified bentonites with excess NaBH<sub>4</sub> results in formation of intralayer Pd clusters or interdendrite Pd clusters (Scheme 3) on CP–bentonite and DAEP–bentonite, respectively. Evidence for this reduction comes from the immediate change in solid color.



**Scheme 1.** Synthesis of 3,3'-(dodecylazanediyl)bis(N-(2-(2-aminoethylamino)ethyl) propanamide).

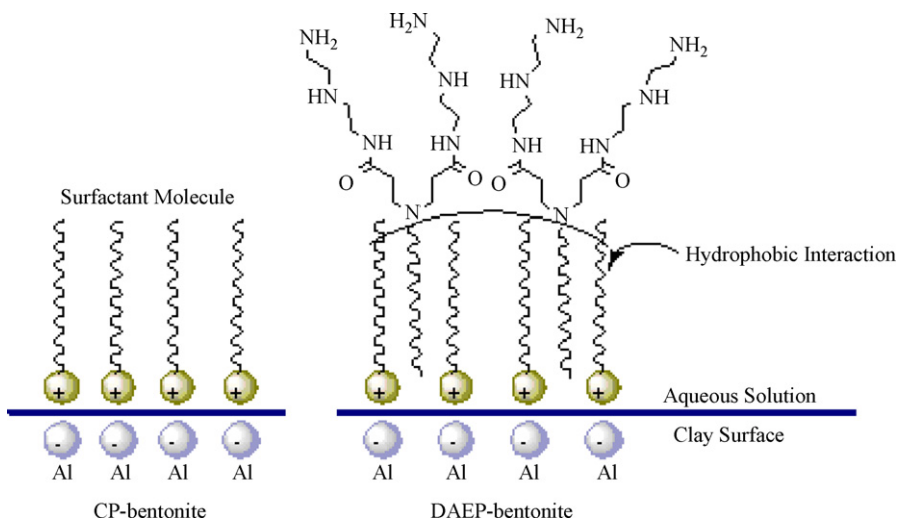
#### 2.3.4. General procedure for oxidation of ethyl benzene

A 25 mL round bottom flask was charged with 1 mmol of ethyl benzene, 0.03 g (0.021 wt% Pd) of catalyst, and the amount of oxidant (0.42 mL of 80% tert-butyl hydroperoxide in 1,2-dichloroethane), and placed in a thermostatic oil bath and fitted with water cooled condenser. The reaction mixture was stirred at reflux temperature (80 °C) for 24 h. The progress of the reaction was monitored by gas chromatography (Agilent technologies 6890N, HP-50 capillary column). Finally, the catalyst was filtered off and washed with ethyl acetate. The filtrate and washings were collected. Finally, the products were analyzed using GC–MS (Shi-

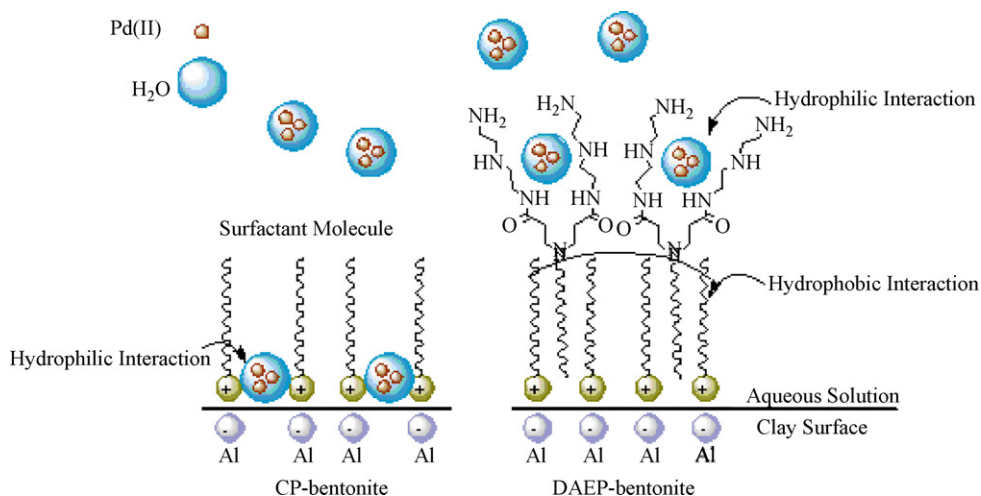
madzu QP 5000; DB 1 column). Identification of products was done by comparing the GC retention times of expected products with those of standard samples. Leaching experiments were carried out in order to prove the heterogeneous character of the reactions. In representative tests, the catalyst was filtered out and the filtrate was analyzed for Pd content using inductively coupled plasma (ICP).

#### 2.3.5. General procedure for the electrochemical measurements

**2.3.5.1. Apparatus.** Cyclic voltammetry (CV) and electrochemical impedance spectroscopy (EIS), were performed in an analytical system, Autolab with PGSTAT 12 (Eco Chemie B.V., Utrecht, The



**Scheme 2.** Model for the sorption of surfactant on the clay surface.



**Scheme 3.** A model of modification of clay surface by surfactant and preparation of Pd nanoparticles.

**Table 1**

Characterization of clay modified monolayer with CP and then modified bilayer with DAEP.

Entry	Support	Composition				Amount of CP (mmol m <sup>-2</sup> ) <sup>c</sup>	Amount of CP + DAEP (mmol m <sup>-2</sup> ) <sup>d</sup>
		N (%)	C (%)	H (%)	C/N		
1	CP-bentonite <sup>a</sup>	0.27	1.75	1.44	6.48	3.04 × 10 <sup>-5e</sup>	
2	DAEP-bentonite <sup>b</sup>	1.69	3.55	1.68	2.10	3.17 × 10 <sup>-5f</sup>	2.93 × 10 <sup>-5f</sup>

<sup>a</sup> Bentonite with monolayer CP coverage.

<sup>b</sup> Bentonite modified with CP and DAEP.

<sup>c</sup> Determined by elemental analysis.

<sup>d</sup> Determined by back titration with NaOH [17].

<sup>e</sup> Amount of CP on the bentonite for preparation of monolayer modified bentonite (CP-bentonite).

<sup>f</sup> Amount of DAEP on the DAEP-bentonite.

Netherlands). For impedance measurements, a frequency range of 100–0.10 Hz was employed. The AC voltage amplitude used was 5 mV, and the equilibrium time was 10 min. A conventional three-electrode cell assembly consisting of a platinum wire as an auxiliary electrode and an Ag/AgCl (KCl<sub>sat</sub>) electrode as a reference electrode was used. The working electrode was either a carbon nanotube paste electrode modified with Pd (0) and Pd (II). A pH-meter (Corning, Model 140) with a double junction glass electrode was used to check the pH of the solutions.

**2.3.5.2. Preparation of the electrode.** Supported nanoparticles (0.1 g) were dispersed in diethyl ether and hand mixed with 70-times their weight of graphite powder and 20-times their weight of carbon nanotube in a mortar and pestle. The solvent was evaporated by stirring. Using a syringe, paraffin was added to the mixture and mixed well for 20 min until a uniformly wetted paste was obtained. The paste was then packed into a glass tube. Electrical contact was made by pushing a copper wire down the glass tube into the back of the mixture. When necessary, a new surface was obtained by pushing an excess of the paste out of the tube and polishing it on a weighing paper.

### 3. Results and discussion

#### 3.1. Synthesis of bentonite-supported dendrimer–palladium complex

DAEP-dendrimer was immobilized on a modified bentonite starting from bentonite with monolayer cetyl pyridinium cation coverage (CP-bentonite). The scheme of the process is shown in Scheme 2. Immobilization of DAEP proceeded smoothly on the modified bentonite. This can be observed from the adsorption

isotherm of DAEP on modified bentonite with monolayer coverage of CP-bentonite (Fig. 1). From the estimation of amino groups and CHN analysis (Table 1), it was found that the final modified bentonite contained 3.35 mmol of DAEP per gram of the final solid. Thus, there are 6.7 mmol of primary amine groups, 6.7 mmol of secondary amino groups, 3.35 mmol of tertiary amine, and 6.7 mmol of amide groups per gram of the final solid. This final modified bentonite was designated as DAEP-bentonite as mentioned before.

Complexation behaviour of Pd (II) ions and Pd (0) with the immobilized dendrimer was studied. In this regard, 0.5 g of the DAEP-bentonite was dispersed in 100 mL of dry *n*-hexane overnight. The reason for choosing *n*-hexane as the medium was that DAEP-bentonite, swells very easily in a non-polar solvent. In the next step, 100 µL of a PdCl<sub>2</sub> solution (10<sup>-2</sup> M) was added during 10 days in 10 steps (10 µL × 10 µL). This is because the dendrimeric head of the DAEP was more solvated in polar solvent, in this case

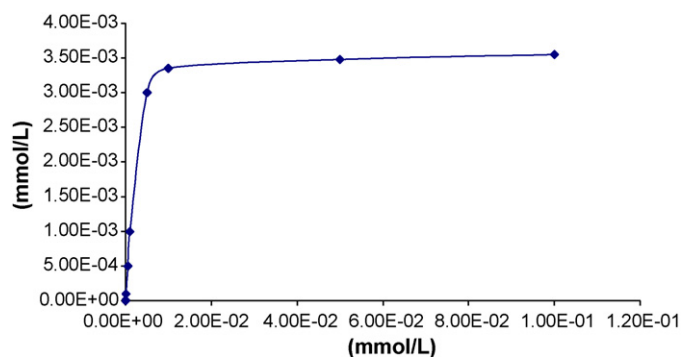


**Fig. 1.** Isotherm of adsorption against concentration of DAEP on modified bentonite with monolayer coverage of CP at room temperature.

**Table 2**

Specific surface area and pore volume for bentonite, modified bentonite and bentonite with palladium nanoparticle.

Entry	Catalyst	Metal content (wt%)	$S_{\text{BET}}$ ( $\text{m}^2 \text{g}^{-1}$ )	$V_p$ ( $\text{cm}^3 \text{g}^{-1}$ )
1	Na-bentonite		124	0.051
2	CP-bentonite <sup>a</sup>		26	0.102
3	DAEP-bentonite <sup>b</sup>		43	0.074
4	CP-bentonite-Pd (II)	0.021	34	0.105
5	CP-bentonite-Pd (0)	0.021	34	0.094
6	DAEP-bentonite-Pd (II)	0.021	51	0.079
7	DAEP-bentonite-Pd (0)	0.021	75	0.060

<sup>a</sup> Bentonite with monolayer CP coverage.

<sup>b</sup> Bentonite modified with CP and DAEP.

water, and so the ligand and metal ions were in a more interacting state, which facilitated the metal intake. To prepare Pd (0) complexes 100 fold excess of  $\text{NaBH}_4$  aqueous solution was applied [18]. This kind of behaviour by dendrimers under homogenous conditions was previously reported [19]. The amount of palladium ions attached on the immobilized dendrimeric ligand under various conditions is given in Table 2.

Fig. 2 represents the FTIR spectra of several samples starting from Na-bentonite to immobilized dendrite and after complexation with Pd (II) and Pd (0). The peaks corresponding to the primary amino groups of the dendrite appear at  $3390 \text{ cm}^{-1}$  and  $3344 \text{ cm}^{-1}$

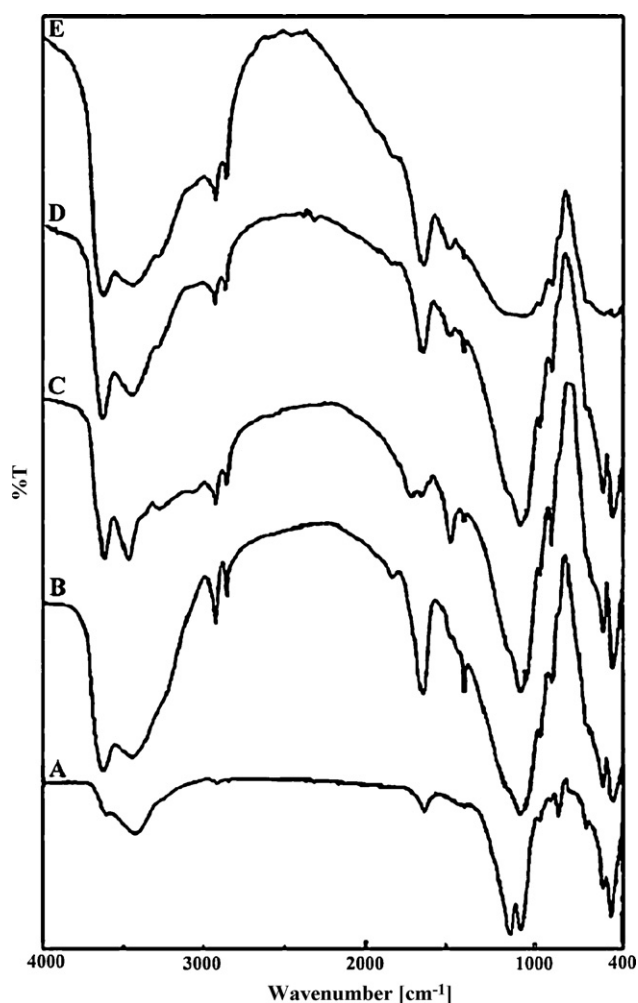


**Fig. 2.** FTIR spectra of (A) Na-bentonite; (B) bentonite modified with a monolayer coverage of CP; (C) DAEP-bentonite; (D) DAEP-bentonite with Pd (II); (E) DAEP-bentonite with Pd (0).

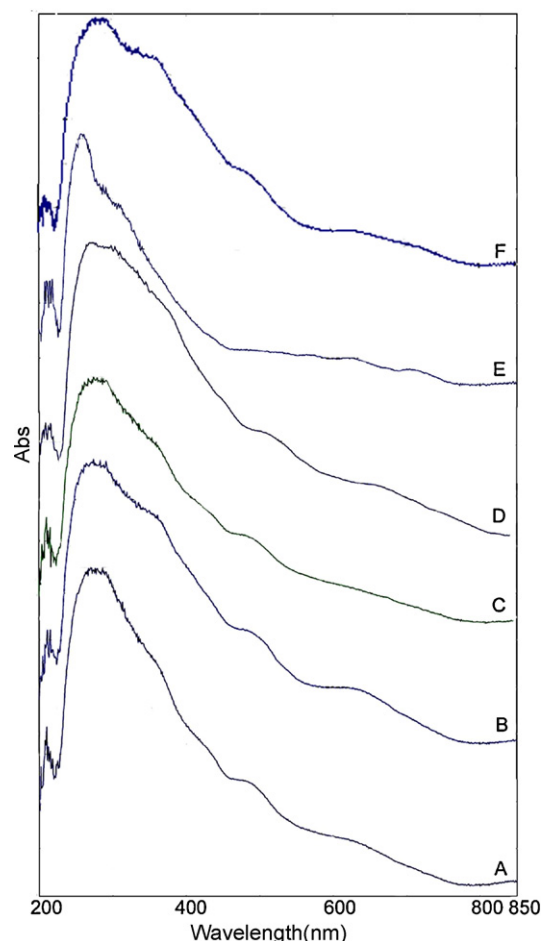


**Fig. 3.** UV-vis spectra of (A) bentonite modified with a monolayer coverage of CP; (B) DAEP-bentonite; (C) CP-bentonite support with Pd (II); (D) CP-bentonite support with Pd (0); (E) DAEP-bentonite with Pd (II); (F) DAEP-bentonite with Pd (0).

which shifted to  $3358 \text{ cm}^{-1}$  and  $3300 \text{ cm}^{-1}$  after complexation with the metal, respectively. This shift is due to participation of the primary amino groups in forming coordination bonds with the metal. There is no change in the band corresponding to the amide groups; this means that the amide groups do not take part in complexation. The electronic spectrum of the complex showed a broad band at  $450 \text{ nm}$ , which may be due to the charge transfer transition, and a band at  $650 \text{ nm}^{-1}$  due to first excited state transition. Complexes of the types  $[\text{PdL}_4]^{2+}$  and  $[\text{PdL}_2\text{Cl}_2]$  can be assigned to the clusters of the encapsulated Pd (II) ions, and probably complexes of the type  $[\text{Pd}^0\text{L}_2\text{Cl}]^-$  [20] could be produced after reduction (Fig. 3). Clearly, complex formation between the metal and amino groups of various branches of the same dendrite is possible.

Transmission electron microscopy (TEM) images (Fig. 4) clearly show that Pd encapsulated particles are nearly monodisperse and that their shape is spherical. The metal particle diameters are less than  $10 \text{ nm}$ .

Table 2 gives the specific surface area and the pore volume data of the immobilized palladium nanoparticles on DAEP-bentonite. Modification of bentonite with cetyl pyridinium bromide as a monolayer decreased the specific surface area. Interestingly, by adding DAEP surfactant to the monolayer modified bentonite to obtain bilayers modified bentonite, the specific surface area increases which might be reasonable, because the hydrophilic head of the DAEP molecules have a water solvation core and one expect that it swells the bentonite to some extent. By loading these modified bentonites with Pd (II) and Pd (0),



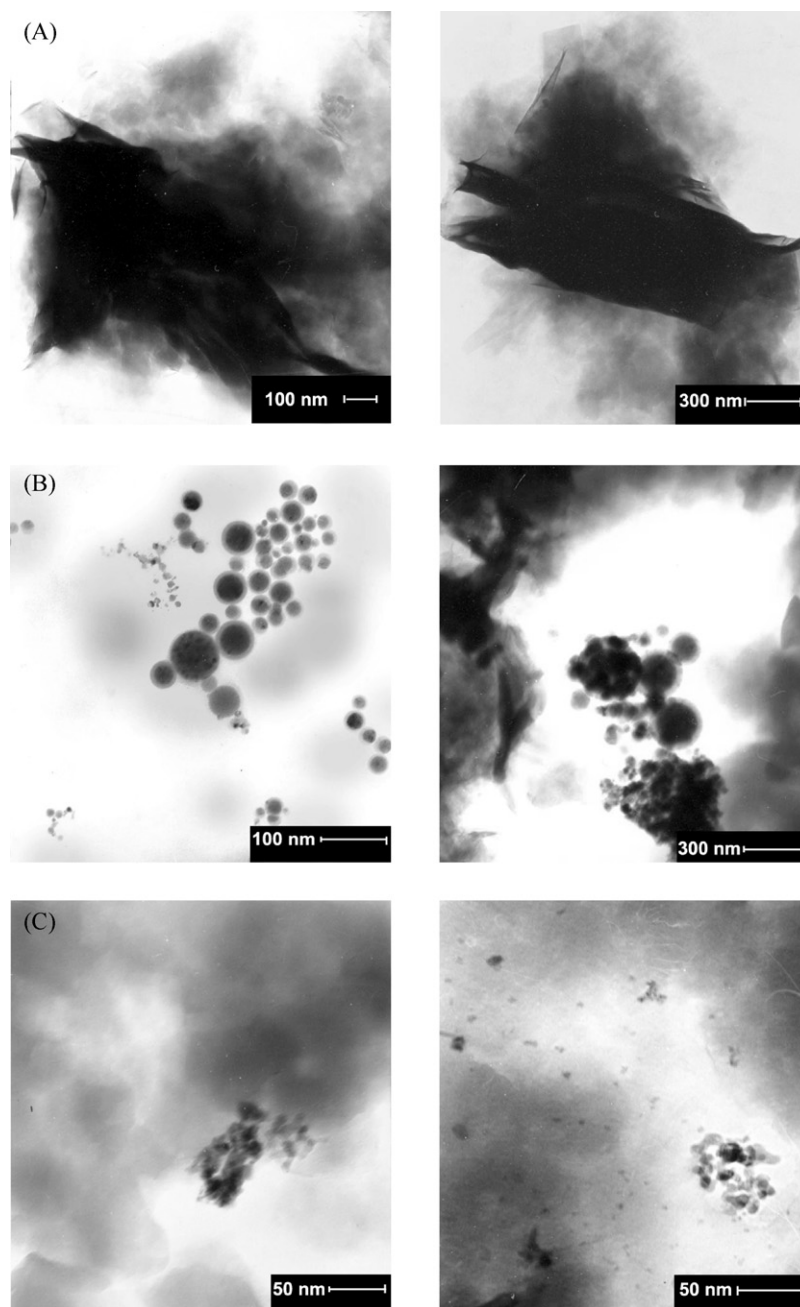


**Fig. 4.** TEM image of (A) immobilized DAEP on modified bentonite with a monolayer coverage of CP; (B) DAEP-bentonite with Pd (II); (C) DAEP-bentonite with Pd (0).

it is plausible to observe an increase in the specific surface area.

The XRD patterns (not shown) of the air-dried surfactant complexes with clay (air humidity, 59%) shows that at the first step of modification with CP, a peak corresponding to  $d(001)$  of 1.32 nm is found, and after loading the bentonite with monolayer surfactant coverage with DAEP, the interlamellar distances do not change. This suggests that DAEP cannot penetrate into interlamellar spaces, and just occupy the edges and the pores.

Scanning electron microscope images of the modified bentonites with or without palladium nanoparticles are shown in Fig. 5. Palladium nanoparticles had a strong influence on the particle structure. The modified bentonite before loading with palladium showed a pack type aggregation of the particles completely different from the SEM images of palladium loaded modified bentonites.

Palladium nanoparticles seem to change the porosity of the aggregated particles.

### 3.2. Synthesis of palladium nanoparticles and nanotubes on surfactant modified bentonite

The sorption of cationic surfactant on a negatively charged surface involves both cation exchange and hydrophobic bonding. At low loading levels, surfactant monomers are retained by ion exchange and eventually form a monolayer. At this stage, by suspending the modified bentonite in an organic solvent such as *n*-hexane, and then adding water to this mixture, water molecules will try to find a site on the surface of the bentonite, especially in places where electrostatic charges exist. One would expect that these electrostatic charges develop where the negative charges of the surface have interaction with the polar head of the surfactant.

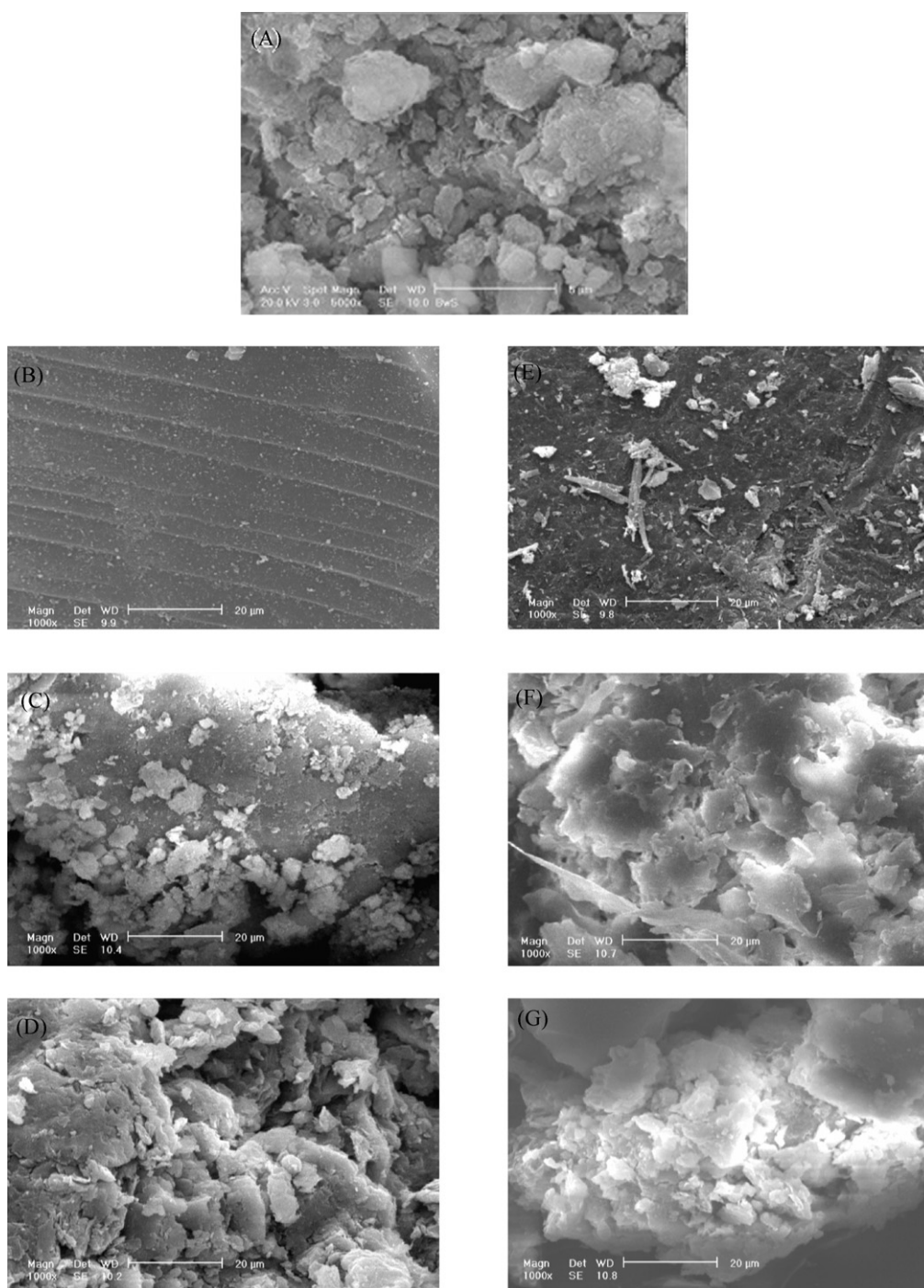


**Fig. 5.** SEM image of (A) Na-bentonite; (B) bentonite modified with a monolayer coverage of CP; (C) CP-bentonite support with Pd (II); (D) CP-bentonite support with Pd (0) (E) DAEP-bentonite; (F) DAEP-bentonite with Pd (II); (G) DAEP-bentonite with Pd (0).

Therefore, by adding palladium solution to the suspended bentonite in *n*-hexane, and depending on the size of the added aqueous solution (in each step, 10  $\mu$ L), separate aqueous pools are formed on the surface. The size of the created water pools exclusively determines the size of the palladium chloride clusters.

Fig. 6 represents the FTIR spectra of various samples starting from Na-bentonite to CP-bentonite and after loading with Pd (II) and Pd (0). All characteristic peaks exist but give the vibrations of organic moieties in the spectra of CP-bentonite, and modified bentonite with palladium nanoparticles compared with Na-bentonite. The vibrations between 2850  $\text{cm}^{-1}$  and 2960  $\text{cm}^{-1}$  are assigned to the asymmetric and symmetric stretching vibrations of  $-\text{CH}_3$  and

$-\text{CH}_2$  units, and the absorption band appeared between 1000  $\text{cm}^{-1}$  and 1260  $\text{cm}^{-1}$  are assigned to the Si–O–Si stretching vibrations. The electronic spectrum of the Pd (0) hybrid material is clearly similar to the electronic spectrum of monolayer modified bentonite, although the spectrum of Pd (II) shows some charge transfer transitions (Fig. 3).

The specific surface area and the pore volume data for the immobilized palladium nanoparticles and nanotubes on CP-bentonite are reported in Table 2. The BET surface areas of the new materials along with reference Na-bentonite were measured both before and after the addition of palladium. The specific surface area of CP-bentonite decreased when it compared to Na-bentonite, but by

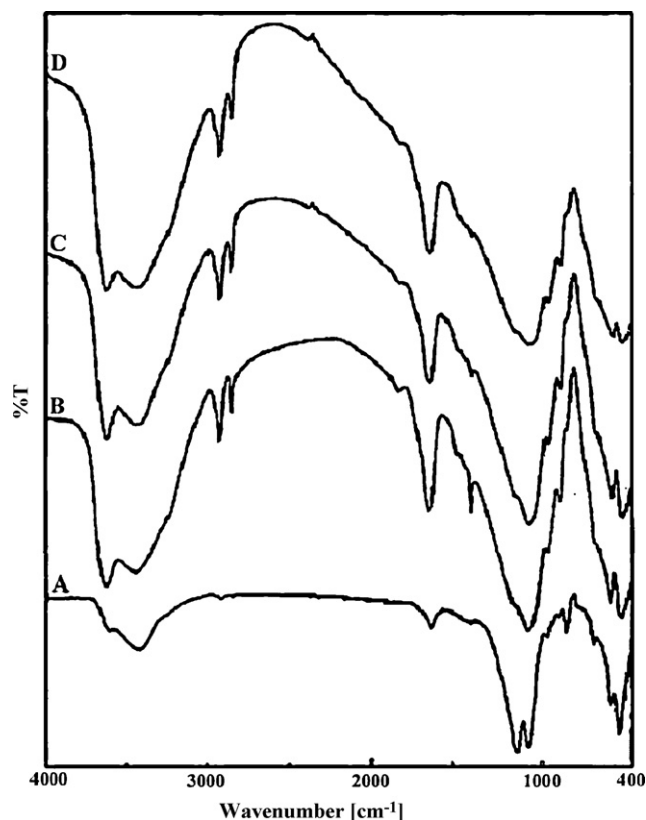


**Fig. 6.** FTIR spectra of (A) Na-bentonite; (B) bentonite modified with a monolayer coverage of CP; (C) CP-bentonite support with Pd (II); (D) CP-bentonite support with Pd (0).

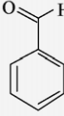
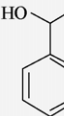
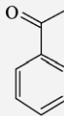
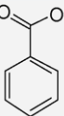
immobilizing palladium the specific surface area of CP-bentonite has increased that might be due to the water pools entered between the layers of bentonite. The presence of Pd (II) nanoparticles or Pd (0) nanotubes in these water pools does not have any significant effect on the surface area.

Transmission electron microscopy (TEM) images (Fig. 7) show that the immobilized palladium nanotubes are empty tubes with a diameter of about 50 nm. Although the preparation of Pd nanoparticles supported on various supports has been reported elsewhere [21], to best of our knowledge there have been no reports on the preparation of palladium nanotubes in the absence of a template.

### 3.3. Oxidation of ethyl benzene catalyzed by DAEP-bentonite-Pd complexes

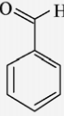
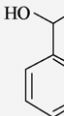
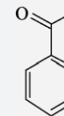
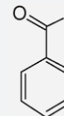
In order to study the catalytic properties of the modified bentonite-supported palladium complexes, we carried out the oxidation of ethyl benzene as a model reaction. Initially, the ratio of substrate to oxidant was changed in the presence of various catalysts (Table 3). The ratio of 1:5 was selected as the best molar ratio of substrate to oxidant, and the DAEP-bentonite-Pd (II) was chosen as the best catalyst. Then, the reaction was carried out at various temperatures (Table 4). The conversion was increased to about 92% at reflux conditions. By optimization of the amount of catalyst and the reaction temperature, the time (Table 5) was also optimized. After completion of the reaction, the catalyst was recovered easily, and after washing with water it can be reused without any difficulty. A positive dendrite effect was observed, when we compared the catalytic efficiency of the DAEP-bentonite-Pd complexes with the palladium catalyst immobilized on bentonite modified with monolayer coverage of CPB surfactant (Table 6). Better results were obtained by DAEP-bentonite-Pd (II) complex. This can be explained if we consider that, with DAEP on the surface of modified bentonite, it prevents the metal leaching and thereby increases the stability

**Table 3**  
Effect of the amount of catalyst, DAEP-bentonite with Pd (II), in oxidation of ethyl benzene.

Entry	Amount of catalyst (g)	Conversion (%)	Selectivity (%)			
						
1	0.00	0.0				
2	0.01	86.9	4.6	15.2	66.5	13.7
3	0.03	92.3	0.6	5.4	93.5	0.5
4	0.05	86.8	0.1	7.4	90.7	0.9
5	0.07	85.3	1.1	0.4	76.9	21.6

Reaction conditions: 80% TBHP; EB:TBHP (mol ratio) = 1–5; time 24 h, temperature = reflux, without solvent.

**Table 4**  
Effect of temperature on the catalytic activity of DAEP-bentonite with Pd (II) in oxidation of ethyl benzene.

Entry	Temperature (°C)	Conversion (%)	Selectivity (%)			
						
1	25	3.6	42.6	7.1	27.1	23.2
2	40	5.5	33.1	8.5	42.6	15.8
3	50	8.8	22.0	10.9	58.9	8.2
4	60	21.4	4.3	15.6	78.7	1.4
5	Reflux	92.3	0.6	5.4	93.5	0.5

Reaction conditions: catalyst weight = 0.03 g; 80% TBHP; EB:TBHP (molar ratio) = 1:5; time 24 h, without solvent.



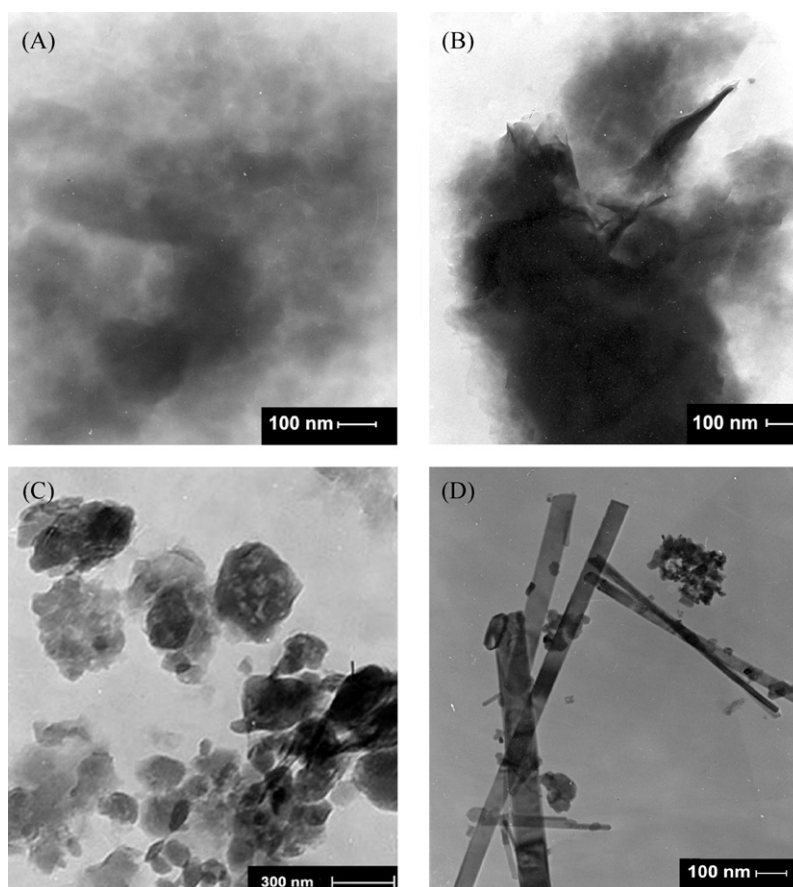


**Fig. 7.** TEM image of (A) Na-bentonite; (B) bentonite modified with a monolayer coverage of CP; (C) CP-bentonite support with Pd (II); (D) CP-bentonite support with Pd (0).

of the catalyst. The catalytic sites of the DAEP-bentonite may work in a cooperative manner due to the peculiar structure of the dendrimeric head of the DAEP, which makes the DAEP-bentonite-Pd complex more efficient catalyst. In addition, the hydrophilic tail of the DAEP acts as a spacer between the support and the catalytic site, which reduces the steric factors offered by the support to some extent. This effect cannot be seen by the CP-bentonite-Pd complex and so it acted as a less efficient catalyst compared to DAEP-bentonite-Pd complex.

The results of reusability of the best catalyst are summarized in Table 7. The catalyst obtained after the first reaction was used in the subsequent runs after washing with ethyl acetate and drying. The catalyst remained active for the next few cycles. There was some drop in the activity of the catalyst, and the metal leaching may be the reason for the drop in activity. Although practically the catalyst

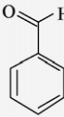
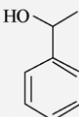
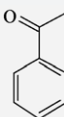
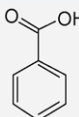
was active after the fifth cycle, but the drop in activity and metal leaching may be due to the partial decomposition of the dendritic ligand due to prolonged exposure to an oxidizing atmosphere. FTIR analysis of the catalyst before and after the reaction showed that the intensity of the band at  $1660\text{ cm}^{-1}$  due to amide group started decreasing; this indicates a possible decomposition of the DAEP backbone during the course of the reaction. After the fifth cycle, the catalyst lost about one third of its activity.

#### 3.4. Electrochemical study using carbon nanotube paste electrode

We used cyclic voltammetry (CV) and electrochemical impedance spectroscopy (EIS) to study the electrochemical behaviour of the prepared nanoparticles at the surface of carbon paste electrode. Fig. 8 shows cyclic voltammogram of Pd (0) and

**Table 5**

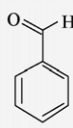
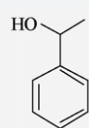
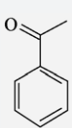
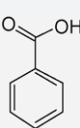
Effect of time on the catalytic activity data in the oxidation of ethylbenzene with DAEP-bentonite-Pd (II).

Entry	Time (h)	Conversion (%)	Selectivity (%)			
						
1	1	24.7	33.2	9.4	41.3	16.1
2	4	36.3	29.3	12.2	46.1	12.4
3	6	47.3	25.1	14.6	47.0	13.3
4	12	59.4	29.8	11.8	30.3	28.1
5	24	92.3	0.6	5.4	93.5	0.5

Reaction conditions: catalyst weight = 0.03 g; 80% TBHP; EB:TBHP (molar ratio) = 1:5; reflux, without solvent.

**Table 6**

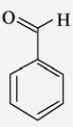
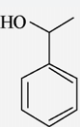
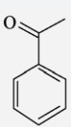
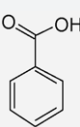
Effect of the EB:TBHP molar ratio on the catalytic activity of palladium catalysts in oxidation of ethyl benzene.

Entry	Catalyst	EB:TBHP (mol)	Conversion (%)	Selectivity (%)			
							
1	CP-bentonite-Pd (II)	1:2	29.5	49.2	12.3	37.0	1.5
2	CP-bentonite-Pd (II)	1:3	21.3	37.0	11.0	45.9	6.1
3	CP-bentonite-Pd (II)	1:4	23.5	38.3	6.4	38.2	17.1
4	CP-bentonite-Pd (0)	1:3	20.6	18.5	23.8	53.2	4.5
5	DAEP-bentonite-Pd (II)	1:1	36.9	4.5	2.8	92.6	0.1
6	DAEP-bentonite-Pd (II)	1:2	40.3	10.8	24.6	59.9	4.6
7	DAEP-bentonite-Pd (II)	1:3	51.6	4.3	27.4	65.1	3.2
8	DAEP-bentonite-Pd (II)	1:4	76.3	1.8	10.9	86.3	1.0
9	DAEP-bentonite-Pd (II)	1:5	92.3	0.6	5.4	93.5	0.5
10	DAEP-bentonite-Pd (0)	1:3	22.4	16.2	6.6	73.5	3.7

Reaction conditions: catalyst weight = 0.03 g; 80% TBHP; time 24 h, reflux, without solvent.

**Table 7**

Activity of recycled catalyst, DAEP-bentonite with Pd (II), in oxidation of ethyl benzene.

Entry	Cycle	Conversion (%)	Selectivity (%)			
						
1	1	92.3	0.6	5.4	93.5	0.5
2	2	64.1	8.9	9.3	80.2	1.6
3	3	68.7	9.1	6.9	82.7	1.2
4	4	61.2	5.6	4.2	88.7	1.5
5	5	59.0	8.5	8.6	81.5	1.3
6	6	57.0	6.8	9.7	81.9	1.6

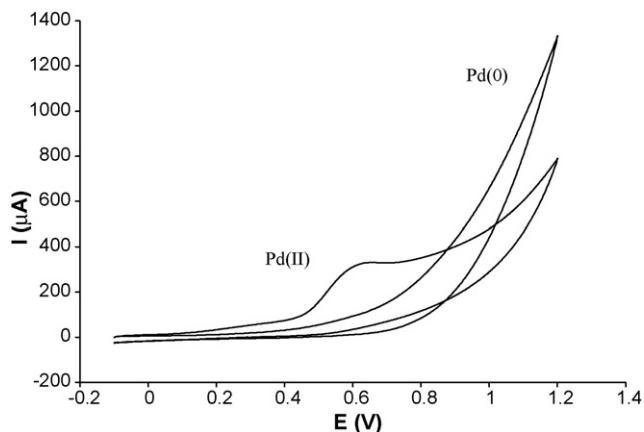
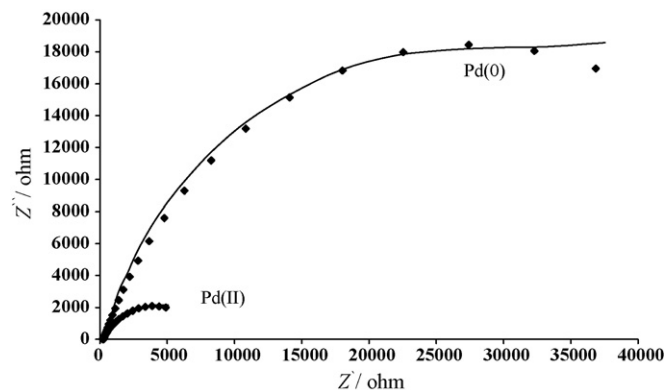
Reaction conditions: catalyst weight = 0.03 g; 80% TBHP; EB:TBHP (molar ratio) = 1:5; time 24 h, reflux, without solvent.

Pd (II) complexes at pH 11.0 in an universal buffer solution. Results show an oxidation peak potential for Pd (II) at 620 mV vs. Ag/AgCl as a reference electrode. We did not observe any oxidation peak for Pd<sup>0</sup> in this potential. Therefore, oxidation of Pd (II) is much faster than of Pd (0) in these conditions, because it oxidizes at a lower potential. One might judge that electron transfer from Pd (II) complex is much easier than that of Pd (0). On the basis of these data one would expect that the Pd (II) complex should be a better catalyst for the oxidation reaction, as experimental data supports.

Electrochemical impedance spectroscopy is a powerful and very informative technique for probing charge transfer properties at the

electrode–solution interface [22]. We have used electrochemical impedance spectroscopy to study Pd (0) and Pd (II) complexes to evaluate their charge transfer coefficients. The values of the charge transfer coefficients have direct relation with electron transfer in electro active materials. The compounds with lower charge transfer coefficient are more efficient in redox reactions.

Fig. 9 shows the Nyquist diagrams and bode plots of the imaginary impedance ( $Z_{im}$ ) vs. the real impedance ( $Z_{re}$ ) of the EIS obtained at the carbon nanotube paste electrode which includes Pd (0) (curve a) or Pd (II) (curve b) nanoparticles. They have been recorded at 0.40 V dc-offset in 0.10 mol L<sup>-1</sup> universal buffer (pH 11.0), respectively. Result shows that the charge transfer coefficient

**Fig. 8.** Cyclic voltammogram of Pd (0) and Pd (II) complexes at pH 11.0.**Fig. 9.** Impedance for palladium (0) and (II) nanoparticles at pH 11.0 with  $E_p$  of +0.40 V vs. Ag/AgCl reference electrode.

cient in the presence of Pd (0) complex is bigger than that of the charge transfer coefficient of the Pd (II) complex. Therefore, the Pd (II) complex can contribute easily in oxidation reaction. It is very interesting that these results are in a good accord with data obtained with cyclic voltammetry data, and oxidation of ethyl benzene.

#### 4. Conclusion

In conclusion, palladium complexes of modified bentonite with 3,3'-(dodecylazanediy)bis(N-(2-(2-aminoethylamino)ethyl) propanamide) (DAEP) were prepared and characterized. These complexes were found to be efficient and reusable catalysts for the oxidation of ethyl benzene to acetophenone under desirable conditions. The catalysts remained stable under several reaction conditions. The catalytic activity was higher for the Pd (II) immobilized on modified bentonite with cetyl pyridinium bromide and DAEP in comparison with Pd (0) on the same support. Moreover, the catalytic activity of the Pd (II) and Pd (0) on bentonite with monolayer surfactant coverage was lower than that of the other catalysts. Oxidation was efficient in the presence of tert-butyl hydroperoxide. This may offer new possibilities for the development of efficient catalysts based on dendrimers.

#### Acknowledgments

Thanks are due to the Research Council of Isfahan University of Technology and Center of Excellence in the Chemistry Department of Isfahan University of Technology for supporting of this work. We

would like to thank Professor A.A. Ensafi for his helpful comments in the electrochemical measurements.

#### References

- [1] N. Lane, J. Nanoparticle Res. 3 (2001) 95–103.
- [2] R.F. Service, *Science* 290 (2000) 1526–1527.
- [3] A.I. Kingon, J.-P. Maria, S.K. Streiffer, *Nature* 406 (2000) 1032–1038.
- [4] S. Lloyd, *Nature* 406 (2000) 1047–1054.
- [5] A.T. Bell, *Science* 299 (2003) 1688–1691.
- [6] O. Carp, C.L. Huisman, A. Reller, *Prog. Solid State Chem.* 32 (2004) 33–177.
- [7] M.A. Vannice, D. Poondi, *J. Catal.* 178 (1998) 386–390.
- [8] H. Einaga, S. Futamura, T. Ibusuki, *Environ. Sci. Technol.* 35 (2001) 1880–1884.
- [9] R. Strobel, J.D. Grunwaldt, A. Camenzind, S.E. Pratsinis, A. Baiker, *Catal. Lett.* 104 (2005) 9–16.
- [10] M. Balogh, P. Laszlo, *Organic Chemistry Using Clays*, Springer-Verlag, Berlin, 1993.
- [11] I. Dekany, L. Turi, Z. Kiraly, *Appl. Clay Sci.* 15 (1999) 221–239.
- [12] M. Ghiaci, M.E. Sedaghat, H. Aghaei, A. Gil, *J. Chem. Technol. Biotechnol.* 84 (2009) 1908–1915.
- [13] M. Ghiaci, R.J. Kalbasi, A. Abbaspour, *Colloid Surf. A* 297 (2007) 105–113.
- [14] M. Ghiaci, M.E. Sedaghat, R.J. Kalbasi, A. Abbaspour, *Tetrahedron* 61 (2005) 5529–5534.
- [15] M. Ghiaci, H. Aghaei, S. Soleimani, M.E. Sedaghat, *Appl. Clay Sci.* 43 (2009) 289–295.
- [16] D.W. Ming, J.B. Dixon, *Clay Clay Miner.* 35 (1987) 463–468.
- [17] N. Tsubokawa, H. Ichioka, T. Satoh, S. Hayashi, K. Fujiki, *React. Funct. Pol.* 37 (1998) 75–82.
- [18] F.P. Zamborini, S.M. Gross, R.W. Murray, *Langmuir* 17 (2001) 481–488.
- [19] M.F. Ottaviani, F. Montalti, N.J. Turro, D.A. Tomalia, *J. Am. Chem. Soc.* 101 (1997) 158–166.
- [20] S. Kozuch, S. Shaik, A. Jutand, C. Amatore, *Chem. Eur. J.* 10 (2004) 3072–3080.
- [21] S. Galvagno, A. Donato, G. Neri, R. Pietropaolo, *J. Chem. Technol. Biotechnol.* 51 (1991) 145–153.
- [22] H. Karimi-Maleh, A.A. Ensafi, A.R. Allafchian, *J. Solid State Electrochem.* 14 (2010) 9–15.